JOURNAL OF MATERIALS SCIENCE **35** (2000) 1037–1041

Surface strengthening and toughening of Si_3N_4/TiC layered composite by slip casting

CHIH-HUNG YEH, MIN-HSIUNG HON
Department of Materials Science and Engineering, National Cheng Kung University, Tainan, Taiwan
E-mail: y5521400@ksts.seed.net.tw

Layered composite using monolithic Si_3N_4 as outer layers and Si_3N_4-15v/o TiC as inner core was fabricated by slip casting and pressureless sintering. As the composite is cooled from high sintering temperature, the difference in coefficients of thermal expansion between the constrained inner core and outer layer is expected to establish a compressive surface stress. The existence of this residual stress was verified by theoretical analysis and Vicker's indentation for the samples with various outer layer thickness. The layered composites exhibited greater strength, apparent fracture toughness and damage resistance due to the presence of compressive surface stresses in the layer.

1. Introduction

The TiC particulate with high modulus, hardness and electrical conductivity acting as a second phase dispersoid has been incorporated into monolithic Si_3N_4 to improve not only the fracture toughness but also the electrical conductivity of composite ceramics [1–6].

Substantial enhancement in strength, toughness and damage resistance has been documented in numerous ceramics, such as SiC/AlN [7], Al_2O_3/ZrO_2 [8–14], Si_3N_4/SiC [15–18] and Si_3N_4/TiC [19] by the introduction of compressive surface stress using a material with high coefficient of thermal expansion (C.T.E) or large molar volume as inner layer in comparison to outer layer material. Upon cooling the difference of C.T.E. or molar volume between constrained inner and outer materials thereby creates a compressive surface stress on the outer layer. In order to obtain a desired thickness of outer layers numerous green-forming techniques including die pressing, slip casting, tape casting, as well as dip-coating were used to fabricate layered composites. As Si_3N_4 has a lower C.T.E ($\approx 3.2 \times 10^{-6}/^{\circ}C$) and better oxidation resistance [6] compared to TiC (C.T.E. $\approx 8 \times 10^{-6}/^{\circ}C$), recently, the present authors [19] have utilized the slip casting process to produce a layered composite in Si_3N_4-TiC system which outer layer (Si_3N_4) can envelop the inner core (Si_3N_4-15v/o TiC), as shown in Fig. 1a. It provides a advantageous route to eliminate the orientational problem of compressive surface stress which still exists in the conventional three layers composite (sandwich type) [7–14] formed by die pressing or tape casting.

In order to confirm the existence of residual surface stress, the present study presents a theoretical analysis as well as use Vicker's indentation method [20] on Si_3N_4-TiC layered composites to investigate the compressive surface stress. Besides, the fracture strength, toughness and damage resistance of Si_3N_4-TiC layered samples are also investigated in this study.

2. Experimental

2.1. Raw materials

The powder mixtures of Si_3N_4 (SN-E10, particle size 0.3 μm, UBE, Tokyo, Japan), 5 wt % Y_2O_3 (grade fine C, particle size <1 μm, H.C. Stark, Goslar, FRG) and 2 wt % Al_2O_3 (AKP-20, particle size 0.5 μm, Sumitomo Co. Ltd., Japan) mixed with 15% volume content of TiC particulate (T-1150, particle sizes 10 μm, CERAC, Wisconsin, USA) were used in this study to prepare the outer layer and inner core materials, respectively.

2.2. Slip casting

Aqueous suspension of Si_3N_4/TiC powder mixtures with a solid content of 36v/o using 0.2–0.5 wt % Darvan C (R.T. Vanderbuilt Co., Norwalk, CT) as defloccuant and PH in 9.5–10.5 was prepared by ball milling. The slips were then cast into plaster of Paris molds to make a solid cast bar. When the bodies were cast, they were carefully removed from the molds and dried at room temperature for at least 24 h.

2.3. Sintering and property measurements

Cast specimens were pressureless sintered at 1775 °C for 4 h at 1 atm in flowing N_2 gas in a graphite furnace (FVPHP-R-5, Fujidempa, Japan). Density of the sintered specimens was measured using water immersion method. Specimens of 5 by 0.5 by 0.5 cm in dimension were tested for flexural strength using four-point bending method with the inner and outer spans of 10 and 20 mm, respectively, and a crosshead of 0.5 mm/min. The fracture toughness, K_c, was measured using the indentation method of Anstis *et al.* [21] with a load of 50 kg to ensure that the ratio of the crack radius to half the indent dimension was at least 2.0. The optical microscope was employed for the measurement of indent crack size and the observation of microstructure.

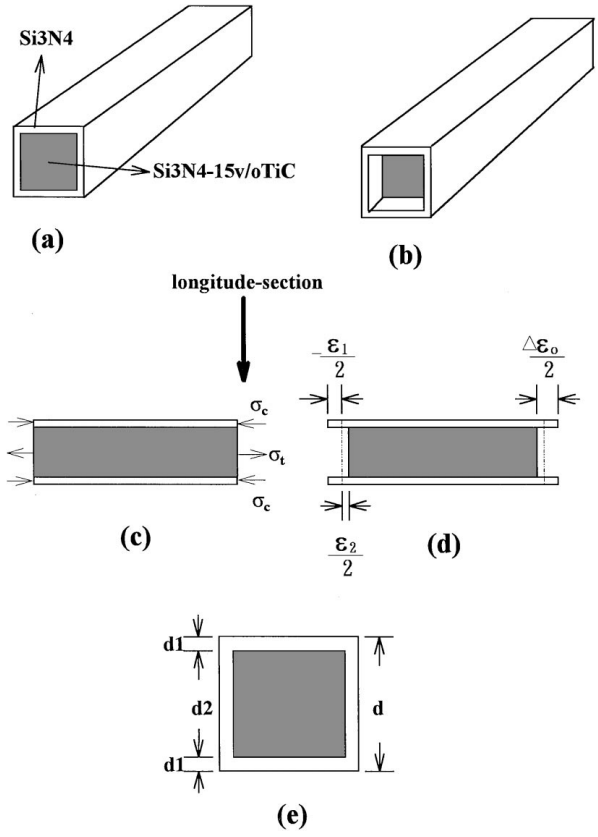

Figure 1 Schematic diagram of a layered composite specimen in Si_3N_4-TiC system, specimen upon cooled strains introduced in constrained (a), (c) and unconstrained (b), (d) outer layers, (e) cross section of (a).

3. Results and discussions

3.1. Theoretical analyses

Fig. 1c shows a schematic diagram of a layered sample with outer layer and inner core thickness of d_1 and d_2, respectively. The total thickness of the sample is $d = 2d_1 + d_2$. If the outer layer and inner core contain monolithic Si_3N_4 and Si_3N_4-TiC composites, respectively, when the sample was cooled from high sintering temperature, the dimension of lower-expansion outer layers is constrained by higher-expansion inner core (Fig. 1d). Therefore, a compressive stress is induced in outer layers compensated by an equivalent tensile stress in inner core.

The magnitude of length is ten times as large as width for layered samples in this study. It is reasonable to assume that the stresses in the direction perpendicular to the interface are very small with respect to the one parallel to the interface. For convenience, neglecting the effect of stresses perpendicular to the interface, the stresses in the outer layers and the inner core parallel to the interface (designated σ_c and σ_t, respectively) can be estimated based on force balance [10], then gives

$$\sigma_c A_1 + \sigma_t A_2 = 0 \tag{1}$$

$$\sigma_c\left(d^2 - d_2^2\right) + \sigma_t d_2^2 = 0 \tag{2}$$

where A_1 and A_2 are the cross-sectional areas of the bar specimen, for outer layers and inner core, respectively. The Poisson's ratio (υ) is assumed to be the same for the inner core and outer layers. In terms of moduli E_1 and E_2, strains ε_1 and ε_2 in the outer layer layers and inner core. Equation 2 can be rewritten as

$$\frac{\varepsilon_1 E_1}{1-\upsilon}\left(d^2 - d_2^2\right) + \frac{\varepsilon_2 E_2}{1-\upsilon} d_2^2 = 0 \tag{3}$$

The free expansion of outer layer relative to the inner core (Fig. 1e) in the direction parallel to the interface is $\Delta\varepsilon_0$. Also

$$-\varepsilon_1 + \varepsilon_2 = \Delta\varepsilon_0 \tag{4}$$

From Equations 3 and 4, and neglecting the minimal difference of moduli between inner core and outer layers, the corresponding stresses are given by

$$\sigma_c = \frac{\varepsilon_1 E_1}{1-\upsilon} = \frac{-\left(E_1 E_2 d_2^2 \Delta\varepsilon_0\right)}{(1-\upsilon)\left[E_1\left(d^2 - d_2^2\right) + E_2 d_2^2\right]}$$

$$= \frac{-E\Delta\varepsilon_0 (d_2/d)^2}{1-\upsilon} \tag{5}$$

$$\sigma_t = \frac{\varepsilon_2 E_2}{1-\upsilon} = \frac{E_1 E_2 \Delta\varepsilon_0\left(d^2 - d_2^2\right)}{(1-\upsilon)\left[E_1 d^2 + d_2^2\left(E_2 - E_1\right)\right]}$$

$$= \frac{-E\Delta\varepsilon_0 [1 - (d_2/d)^2]}{1-\upsilon} \tag{6}$$

The compressive stress is proportional to the normalized inner core thickness $(d_2/d)^2$. Using monolithic Si_3N_4 and Si_3N_4-15v/o TiC as outer layers and inner core, respectively, the coefficients of thermal expansion of monolithic Si_3N_4 and Si_3N_4-15v/o TiC are approximately $3.2 \times 10^{-6}/^\circ$C and $3.92 \times 10^{-6}/^\circ$C, respectively. The creep rate of Si_3N_4-TiC is significant above 1350 °C [22]. For ΔT = 1350–25 °C = 1325 °C, $\Delta\varepsilon_0$ can be estimated by $\Delta\alpha\Delta T$ [7] = $(3.92 - 3.2) \times 10^{-6}/^\circ\text{C} \times 1325\,^\circ\text{C} = 9.54 \times 10^{-4}$. Table I gives the calculated values of compressive stress in the outer layers (assuming a sharp transition in residual stresses at the interface) and the corresponding tensile stress in the inner core using E = 300 GPa and υ = 0.28. Obviously, the predicted compressive residual stress, σ_c, increase with increasing the values of $(d_2/d)^2$. By the same token, σ_c increases with decreasing the outer layer thickness d_1 for a fixed total thickness.

3.2. Residual surface compression stress measurements

Fig. 2 shows indents on outer surfaces of layered composite and a monolithic sample respectively. The

TABLE I Calculated residual stresses for Si_3N_4-TiC layered samples, based on Equations 5 and 6

d_1 (μm)	d_2 (μm)	$(d_1/d_2)^2$	σ_c (MPa)	σ_t (MPa)
250	4500	0.81	−322	76
500	4000	0.64	−254	143
750	3500	0.49	−195	203
1000	3000	0.36	−143	254
1250	2500	0.35	−99	297

Total thickness of the layered bar, $d = 2d_1 + d_2$, is 5 mm.

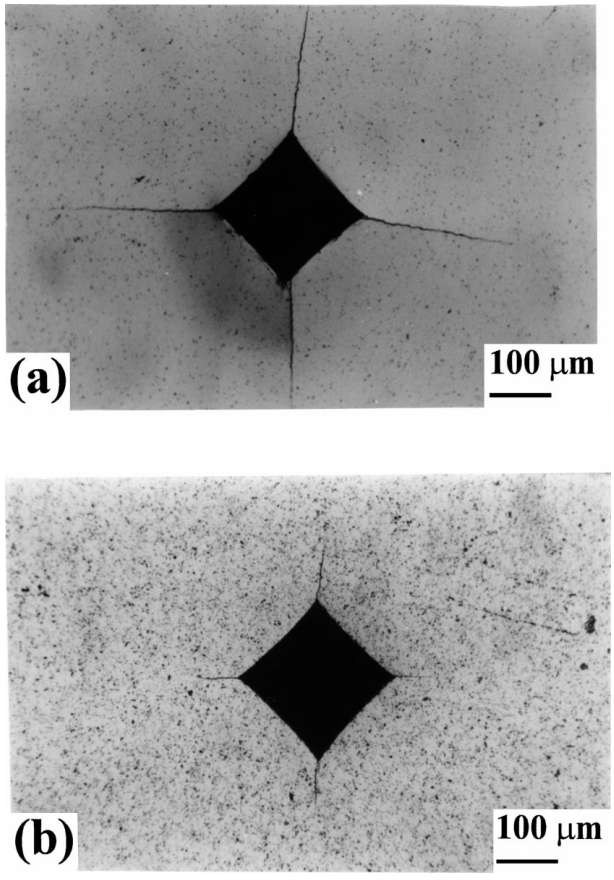

Figure 2 SEM micrographs of Vickers indentation of a load of 500 N on the surface of (a) monolithic Si_3N_4 and (b) Si_3N_4-TiC layered sample with 250 mm outer layer thickness.

influence of residual stresses is apparent on the crack sizes. For an indent load of 50 kg (≈500 N); crack size in the Si_3N_4-TiC layered composite ($d_1 = 250\,\mu$m) and monolithic Si_3N_4 are respectively 0.22 and 0.34 mm. It is assumed the flaw is half pennyshaped and its depth is much smaller than the outer layer thickness and the crack pattern mainly is influenced by the stress state. The existence of compressive residual stress in a surface layer can be approximated by Vicker's indentation method [20, 23–25]

$$\sigma_c = 1/2\sqrt{\pi/C}\left(K_c - K_c^0\right) = 1/2\sqrt{\pi/C}\left(\frac{\chi p}{C^{3/2}} - \frac{\chi p}{C_0^{3/2}}\right) \qquad (7)$$

where P is indent load; K_c^0, K_c and C_0, C are apparent fracture toughness and indent crack lengths for monolithic Si_3N_4 and Si_3N_4-TiC layered composite, respectively; χ is a dimensionless field intensity parameter. With K_c^0 of Si_3N_4 is 5.7 MPa · $m^{1/2}$, the χ is estimated to be 0.0726. The measured C_0 and C incorporated the value of χ insert into Equation 7, thus compressive residual stress can be obtained. Fig. 3 is the comparisons of measured values (Equation 7) and theoretically calculations (Equation 5) of σ_c as a function of normalized inner layer thickness. The measured values are in agreement with calculated values. For example, the magnitude of calculated value of σ_c is 322 MPa similar to the measured value of 311 MPa for Si_3N_4-TiC layered composite with a 250 μm thickness of Si_3N_4 outer layer. The presence of residual surface compression stress is expected to not only enhance the damage resistance but also strengthen materials.

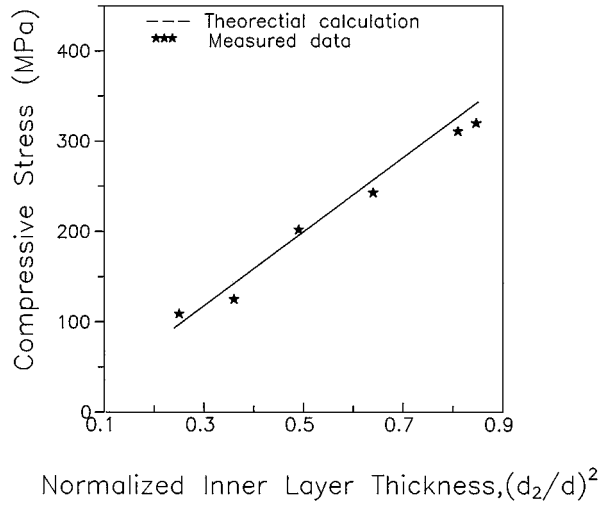

Figure 3 The comparisons of σ_c for experimental measurement and theoretical calculation (Equation 5) as function of normalized inner layer thickness, $(d_2/d)^2$.

3.3. Mechanical properties

Fig. 4 shows the apparent fracture toughness K_c as function of normalized inner layer thickness $(d_2/d)^2$ as derived from Vickers indentation measurements. The materials for outer layer (Si_3N_4) and inner core (Si_3N_4-15v/oTiC) are characterized by $K_c^0 = 5.7$ and 5.1 MPa · $m^{1/2}$, respectively, while apparent fracture toughness K_c attains significantly higher values for all layered composites, suggesting the presence of residual stresses. K_c of layered composite increases with increasing $(d_2/d)^2$, as $(d_2/d)^2$ in the case of 0.64–0.81, K_c is higher than 10 MPa · $m^{1/2}$ increasing above 75% compared to either outer layer or inner core materials.

Fracture strength of layered composites is dependent on the failure sites, if fracture in bending had

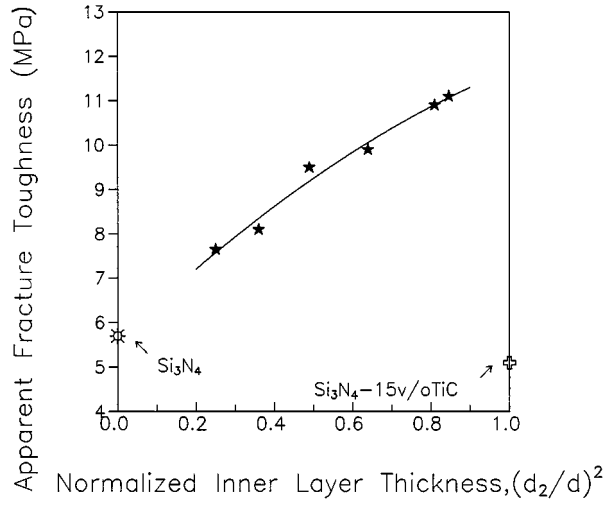

Figure 4 Apparent fracture toughness K_c^0 measured by indentation of sample surface as function of $(d_2/d)^2$.

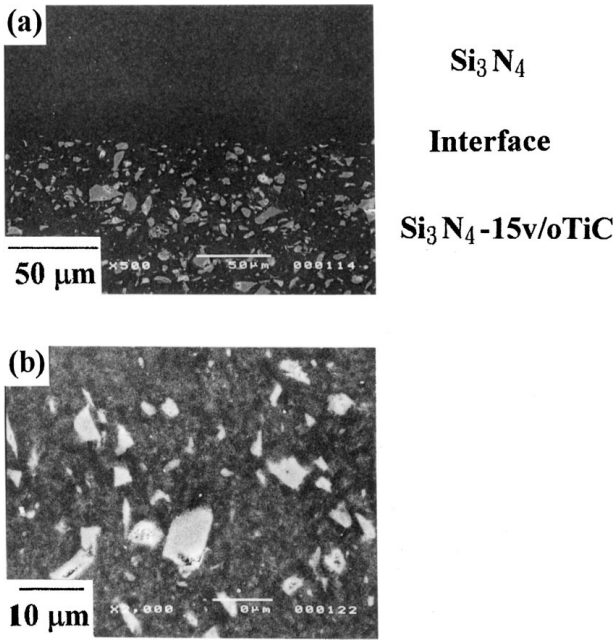

Figure 5 SEM micrography of cross section of (a) interface and (b) inner core of layered sample.

occurred from a surface flaw, the strength would be expected to increase with increasing σ_c [10], in this present work namely increases with increasing $(d_2/d)^2$ Fig. 5 show the microstructure of cross section of layered sample. The interface and different microstructure on outer layer and inner core are clearly visible. The interfacial region is free of any defects such as voids. For inner core, however, it can be found that pores appear nearby interface of TiC and matrix Si_3N_4 and/or interior of TiC particulate. Fig. 6 is the bending strength of Si_3N_4-TiC layered composites as function of $(d_2/d)^2$. The strength of layered composites, however, doesn't increase with increasing $(d_2/d)^2$. The potential failure sites of Si_3N_4-TiC layered composites in the region of either surface or at the interface, however, always make the interpretation of the relationship between fracture strength and $(d_2/d)^2$ complicated and difficult. As in

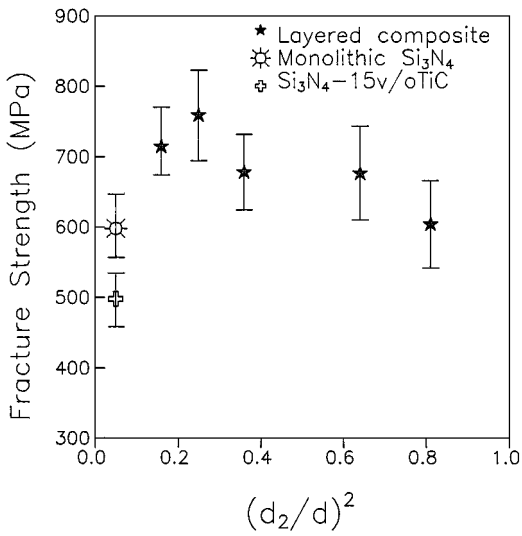

Figure 6 Four-point bending strengths of samples as function of $(d_2/d)^2$.

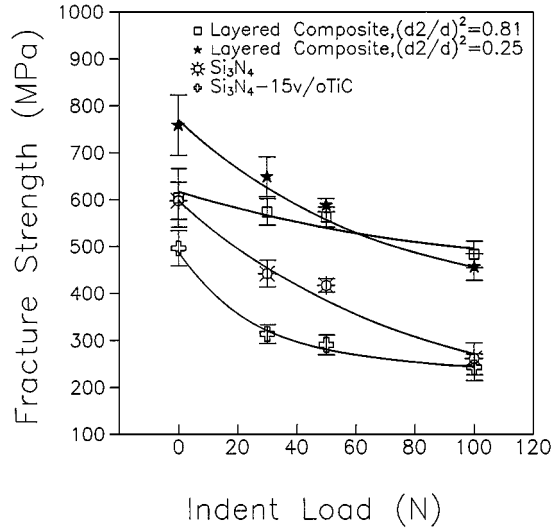

Figure 7 Indentation load dependence of four-point strengths for layered samples, inner core and outer layer materials.

the case of $(d_2/d)^2 = 0.25$ (i.e. $d_1 = 1250$ μm), the obtained fracture strength of Si_3N_4-TiC layered composites is as high as 758 MPa (increasing 52 and 26% in comparison with inner core and outer layer materials, respectively). Compared with the inner core material (Si_3N_4-15v/oTiC composite), Si_3N_4-TiC layered composites show a higher fracture strength in this range of $(d_2/d)^2$ test achieving a strengthening effect.

Fig. 7 is the strengths of samples as function of indentation load. The pre-introduced surface cracks by indentation using various loads act a similar character of various surface flaws which always already exist on the surface of ceramics by contact-induced damage or processing flaw. As can be seen, all of samples decrease in strength with increasing indentation load. Compared with other samples abruptly decreasing in strength with increasing indent loads, Si_3N_4-TiC layered composite with a 250 μm thickness of Si_3N_4 outer layer, $(d_2/d)^2 = 0.81$, decreases in strength only 20% after indent with a load of 100 N due to the presence of 311 MPa surface compression stress. In general, the mechanical properties of ceramics are sensitive to surface flaw, so that the development of a compressive surface stress for a layered composite produced by slip casting technique provides an attractive feature to be resistant to failure from surface flaws as long as the outer layer thickness exceeds the flaw depth.

4. Conclusions

The magnitude of surface compression stresses can be estimated using theoretical analysis and Vicker's indentation method on the Si_3N_4-TiC layered samples with various outer layer thickness. The residual stress increases with increasing normalized inner layer thickness, $(d_2/d)^2$. Si_3N_4-TiC layered samples exhibit a greater apparent fracture toughness and damage resistance compared with outer layer and inner core materials. Samples with higher $(d_2/d)^2$ obtain a larger apparent fracture toughness and damage resistance due to the attribution of higher compressive surface stresses.

Si_3N_4-TiC layered composites show higher fracture strengths in comparison with the inner core material. Samples with 1250 μm of outer layer thickness (i.e. $(d_2/d)^2 = 0.36$) obtain a strength as high as 758 MPa, increasing 52 and 26% in comparison with inner core and outer layer materials, respectively.

References

1. T. MAH, M. G. MENDIRTTA and H. A. LIPSITT, *Amer. Ceram. Soc. Bull.* **60** (1981) 1229.
2. G. ZILBERSTEIN and S. T. BULJAN, in "Advances in Materials Characterization II, Materials Science Research," Vol. 19, edited by R. S. Snyder, R. A. Condrate and P. F. Johnson (Plenum Press, New York, 1985) p. 389.
3. S. T. BULJAN and G. ZILBERSTEIN, in Tailoring of Multiphase and Composite Ceramics, Materials Science Research, Vol. 20, edited by R. E. Tressler *et al.*, (Plenum Press, New York,) 1986, p. 305.
4. F. PENI, J. CRAMPON, R. DUCLOS and B. CALES, *J. Euro. Ceram. Soc.* **8** (1991) 311.
5. J. L. HUNG, H. L. CHIU and M. T. LEE, *J. Amer. Ceram. Soc.* **77** (1994) 705.
6. Y. G. GOGOTSI, *J. Mater. Sci.* **29** (1994) 2541.
7. R. SATHYAMOORTHY and A. V. VIRKAR, *J. Amer. Ceram. Soc.* **75** (1992) 1136.
8. F. F. LANGE, *ibid.* **63** (1980) 38.
9. D. J. GREEN, *ibid.* **66** (1983) C178.
10. A. V. VIRKAR, J. L. HUANG and R. A. CULTER, *ibid.* **70** (1987) 164.
11. R. A. CULTER, J. D. BRIGHT, A. V. VIRKAR and D. K. SHETTY, *ibid.* **70** (1987) 714.
12. A. V. VIRKAR, J. F. JUE, J. J. HANSEN and R. A. CULTER, *ibid.* **71** (1988) C148.
13. J. J. HANSEN, R. A. CULTER, D. K. SHETTY and A. V. VIKAR, *ibid.* **71** (1988) C501.
14. Y. KOBAYASHI and E. KATO, *J. Ceram. Soc. Jpn.* **102** (1994) 609.
15. M. L. TORTI, JR. and D. W. RICHERSON, US Patent no. 3.911.188, (1975).
16. T. ARACHORI and N. IWAMOTO, *J. Ceram. Soc. Jpn (Int. Edn.)* **97** (1989) 1347.
17. D. L. JIANG, J. H. SHE, S. H. TAN and P. GREIL, *J. Amer. Ceram. Soc.* **75** (1992) 2568.
18. P. GREIL, H. G. BOSSEMEYER and A. KLUNER, *J. Euro. Ceram. Soc.* **13** (1994) 159.
19. C. H. YEH and M. H. HON, accepted by *Ceram. Int.* (1996).
20. D. B. MARSHALL and B. R. LAWN, *J. Mater. Sci.* **14** (1979) 2001.
21. G. R. ANSTIS, P. CHANTIKUL, B. R. LAWN and D. B. MARSHALL, *J. Amer. Ceram. Soc.* **64** (1981) 533.
22. F. PENI, J. CRAMPON and R. DUCLOS, *Ceram. Int.* **18** (1992) 413.
23. B. R. LAWN and E. R. FULLER, *J. Mater. Sci.* **19** (1984) 4061.
24. B. R. LAWN, A. G. EVANS and D. B. MARSHALL, *J. Amer. Ceram. Soc.* **63** (1980) 574.
25. M. F. GRUNINGER, B. R. LAWN, E. N. FARABOUGH and JR. J. B. WACHTMAN, *ibid.* **70** (1987) 344.

Received 11 July 1996
and accepted 2 June 1999